




Research Article  
Human and Medical Genetics

# $\Delta$ Np63 $\alpha$ promotes cigarette smoke-induced renal cancer stem cell activity via the Sonic Hedgehog pathway

Yuxiang Zhao<sup>1,2\*</sup>, Nannan Ma<sup>1\*</sup>, Wanngyu Wu<sup>1</sup>, Ying Wu<sup>1</sup>, Wenbo Zhang<sup>1</sup>, Weiwei Qian<sup>1</sup>, Xin Sun<sup>1</sup>   
and Tao Zhang<sup>1</sup>

<sup>1</sup>Anhui Medical University, Second Affiliated Hospital, Department of Urology, Hefei, China.

<sup>2</sup>Anqing 116 Hospital, Department of Urology, Anqing, China.

## Abstract

Cigarette smoke (CS) has been generally recognized as a chief carcinogenic factor in renal cell carcinoma (RCC). The stimulative effect of CS on renal cancer stem cells (RCSCs) has been described previously. The Sonic Hedgehog (SHH) pathway plays an essential role in self-renewal, cell growth, drug resistance, metastasis, and recurrence of cancer stem cells (CSCs). Renal cancer-related gene  $\Delta$ Np63 $\alpha$  is highly expressed in renal epithelial tissues and contributes to the RCSCs characteristics of tumors. The aim of this study was to elucidate the role of  $\Delta$ Np63 $\alpha$  and the SHH pathway on the activity of RCSCs induced by CS through a series of *in vivo* and *in vitro* studies. It was shown that in renal cancer tissues,  $\Delta$ Np63 $\alpha$  and RCSCs markers in smokers are expressed higher than that in non-smokers. RCSCs were effectively enriched by tumor sphere formation assay. Besides, CS increased the expression of RCSCs markers and the capability of sphere-forming *in vitro* and *in vivo*. Moreover, the SHH pathway was activated, and the specialized inhibitor alleviated the promotion of CS on RCSCs.  $\Delta$ Np63 $\alpha$  activated the SHH pathway and promoted CS-induced enhancement of RCSCs activity. These findings indicate that  $\Delta$ Np63 $\alpha$  positively regulates the activity of CS-induced RCSCs via the SHH pathway.

**Keywords:** Cigarette smoke, renal cancer stem cells,  $\Delta$ Np63 $\alpha$ , Sonic Hedgehog signaling pathway.

Received: December 04, 2023; Accepted: April 25, 2024.

## Introduction

Renal cell carcinoma (RCC) is a common urinary malignancy. In 2020, there were about 77410 newly diagnosed cases and 46345 deaths in China and the United States (Xia *et al.*, 2022). About 20%-30% of RCC has metastasis at the first time of diagnosis, and they are mostly resistant to radiotherapy and chemotherapy, leading to abysmal prognosis (Rouprêt *et al.*, 2023). Cancer stem cells (CSCs) are cells in tumors that can self-renew and generate heterogeneous tumor cells, which play a crucial role in the formation and advancement of tumors (Wu *et al.*, 2023). Therefore, exploring the mechanism of renal cancer stem cells (RCSCs) facilitates RCC treatment and prevention.

The Sonic Hedgehog (SHH) signaling pathway plays an essential role in self-renewal, tumor cell growth, drug resistance, metastasis, and recurrence of CSCs (Jeng *et al.*, 2020). Stimulation of the SHH signaling pathway significantly boosted RCC cell proliferation and accelerated the EMT process, which promoted RCC progression (Behnsawy *et al.*, 2013). Downregulation of the SHH pathway could inhibit the proliferation of RCSCs (Li *et al.*, 2019).

Numerous studies have shown that CS is closely related to the occurrence and development of several cancers, such as bladder cancer (Jubber *et al.*, 2023), gastrointestinal cancer (Yuan *et al.*, 2023), and RCC (Znaor *et al.*, 2015). CS could increase the risk of RCC by 50% in male and 20% in female

smokers (Znaor *et al.*, 2015). We have explored the relationship between CS and RCC previously. We found that CS effectively promoted renal CSCs stemness by enhancing tumor sphere formation and increasing the expression of renal CSCs markers (Qian *et al.*, 2018). We also discovered that CS promoted RCC progression by promoting EMT (Zhang *et al.*, 2020).

$\Delta$ Np63 $\alpha$  is a significant regulator in maintaining the characteristics of CSCs. Studies have shown that  $\Delta$ Np63 $\alpha$  is required to regulate the SHH signaling pathway (Cao *et al.*, 2008; Ge *et al.*, 2023). Cao *et al.* (2008) found that overexpression of  $\Delta$ Np63 $\alpha$  in RCC could up-regulate the protein and mRNA levels of the SHH signaling pathway. Dietary diallyl trisulfide inhibited gastric cancer stemness by  $\Delta$ Np63/SHH pathway (Ge *et al.*, 2023). Another study suggests that the IL-6/ $\Delta$ Np63 $\alpha$ /Notch axis plays a vital role in the long-term tobacco smoke exposure-induced acquisition of lung CSC-like properties (Xie *et al.*, 2019). However, the role of  $\Delta$ Np63 $\alpha$  in CS-induced activity acquisition in CSCs remains largely unknown. Therefore, the present study aims to investigate the role of  $\Delta$ Np63 $\alpha$ /SHH signaling pathway in CS-triggered RCSCs and elucidate the underlying molecular mechanism, thereby providing valuable scientific insight for mechanism-oriented intervention research in RCSCs.

## Material and Methods

### Collection of patient samples

All samples were obtained from the Department of Urology, the Second Affiliated Hospital of Anhui Medical University, with the approval of the Ethics Committee of Anhui Medical University and the patient's consent. During

Send correspondence to Xin Sun. Anhui Medical University, Second Affiliated Hospital, Department of Urology, 678 Furong Road, 230032, Hefei, China. E-mail: [m15077916345\\_1@163.com](mailto:m15077916345_1@163.com).

\*These authors contributed equally to the article.

the collection, renal cancer tissues were cut off and stored in the refrigerator at  $-80^{\circ}\text{C}$  immediately, and the data were registered in the specimen bank. All patients had never received radiotherapy, chemotherapy, or targeted therapy. The pathological types were confirmed as clear cell RCC by two pathologists. Besides, smokers possess more than ten years of history. The study was conducted in the Second Affiliated Hospital of Anhui Medical University, Hefei, China, and was approved by the ethics committee of the hospital (No. LLSC20190660). All presentations of case reports have consent for publication.

#### Cigarette smoke extract (CSE) preparation and cell culture

A filter-free 3R4F cigarette (9 mg tar and 0.76 mg nicotine/cigarette, Kentucky, USA) was burned to continuously instill CS at the rate of 5 min one cigarette through a glass syringe containing 10 ml of pre-warmed ( $37^{\circ}\text{C}$ ) serum-free medium. Then the CSE solution was adjusted to pH 7.4 and passed through a filter with a pore size of  $0.22\ \mu\text{m}$ . The solution was then referred to as 100% CSE solution.

Human clear cell renal carcinoma cell lines 786-O and ACHN were purchased from the Cell Bank of the Chinese Academy of Sciences (Shanghai, China). 786-O cells were cultured in RPMI-1640 medium supplemented with 10% fetal bovine serum and 1% penicillin-streptomycin, whereas ACHN cells were cultured in a cell incubator containing 5%  $\text{CO}_2$  at  $37^{\circ}\text{C}$  and 5%  $\text{CO}_2$  at  $37^{\circ}\text{C}$  using MEM medium.

#### Tumor sphere formation assay

786-O, ACHN cells were seeded at 5000 cells/well into 24-well culture plates and cultured with SFM medium. The SFM medium was prepared using DMEM-F12, followed by adding 20 ng/ml EGF, 20 ng/ml bFGF, 5  $\mu\text{g}/\text{ml}$  insulin, and 2% B27 for 5 consecutive days with semi-quantitative fluid exchanges every other day. Different concentrations of CSE were added to each well for 5 consecutive days, and only the number of tumor spheres with a diameter  $>50\ \mu\text{m}$  was counted.

#### Western blot experiments

The treated cells and tissues were lysed in RIPA buffer (Beyotime, Nanjing, China) containing 1% protease inhibitors and phosphatase. Protein concentration was determined by BCA Protein assay kit (Beyotime, Nanjing, China) followed by sodium dodecyl sulfate-polyacrylamide gel electrophoresis (SDS-PAGE) separation and transfer to PVDF membrane. Membranes were blocked with 5% skim milk powder at room temperature for 1 hour and incubated overnight at  $4^{\circ}\text{C}$  with the following primary antibodies:  $\Delta\text{Np}63\alpha$  (13109S, Cell signaling technology, Massachusetts, USA), CD44 (15675-1-AP, Proteintech, Rosemont, IL, USA), Oct4 (60242-1-Ig, Proteintech, Rosemont, IL, USA), SOX2 (11064-1-AP, Proteintech, Rosemont, IL, USA), Gli2 (ab277800, Abcam, Cambridge, UK), Gli1 (ab217326, Abcam, Cambridge, UK), Smo (ab7817, Abcam, Cambridge, UK), Shh (ab53281, Abcam, Cambridge, UK), GAPDH (60004-1-Ig, Proteintech, Rosemont, IL, USA). Then followed by incubating with secondary antibodies. GAPDH was used as an internal control.

#### Quantitative real-time polymerase chain reaction

TRIzol reagent was added to the treated cells for RNA extraction. The concentration was measured at a wavelength of 260 nm, and the cDNA was reverse transcribed according to the kit requirements (NovaBio, Massachusetts, USA) to obtain a concentration of no more than 50 mg/L cDNA. The liquids were then mixed according to the needs of the qPCR kit (NovaBio, Massachusetts, USA) and amplified using a two-step PCR reaction procedure. GAPDH was set as the internal control, and the relative expression of mRNA was calculated according to the  $2^{-\Delta\Delta\text{CT}}$  method.

#### Detection of CD44 positive cells by flow cytometry

The treated cells were picked up and washed twice with precooled PBS solution. CD44 antibody was added, a secondary antibody was added after incubation at room temperature, and after incubation at room temperature in the dark, the cells were washed twice with PBS solution. Finally, the cells were resuspended in 200  $\mu\text{l}$  PBS solution, and the number of CD44 positive cells was detected by computer operation.

#### Cell viability assay

Cells were seeded into 96-well plates at 1000 cells/well density and semiquantitatively changed every other day in the SFM medium. Cell viability was measured using the Cell Counting Kit-8 (Sigma-Aldrich, Shanghai, China) according to the manufacturer's instructions 5 days later.

#### Immunohistochemistry

Paraffin tissue prepared in advance was sectioned on a microtome at a standard of  $4.0\ \mu\text{m}$ . Slides were then deparaffinized in xylene, hydrated in a graded ethanol series, and antigen repaired with citrate buffer. After 30 min block with serum at room temperature, primary antibody ( $\Delta\text{Np}63\alpha$ , 13109S, CST, 1:200; CD44, 15675-1-AP, Proteintech, 1:500) were incubated at  $4^{\circ}\text{C}$  overnight and incubated at room temperature with secondary antibody for 30 min the next day. Cells were then briefly counterstained with diaminobenzidine (DAB), and nuclei were stained with hematoxylin. Finally, the slides were observed under a light microscope.

#### Co-immunoprecipitation

The treated cells were collected, precooled lysate added, lysed sufficiently, and sonicated on ice for fragmentation. The cells were centrifuged at  $14,000 \times g$  for 10 min at  $4^{\circ}\text{C}$ , and 5  $\mu\text{l}$  Protein A and 5  $\mu\text{l}$  Protein G were added to 500  $\mu\text{l}$  of the supernatant. The cells were then centrifuged at  $12,000 \times g$  at  $4^{\circ}\text{C}$  for 1 min, and 1  $\mu\text{g}$  of antibody was added to the lysate. In contrast, IgG, a nonspecific immune homologous antibody, was used as a control and incubated overnight at  $4^{\circ}\text{C}$ . An additional 5  $\mu\text{l}$  Protein A and 5  $\mu\text{l}$  Protein G were added, and the incubation was continued overnight at  $4^{\circ}\text{C}$ . The samples were centrifuged at  $12,000g$  for 1 min and washed with a cleaning solution, followed by centrifugation at  $12,000 \times g$  for 1 min and repeated cleaning three times. 20  $\mu\text{l}$  of loading buffer was added, boiled at  $100^{\circ}\text{C}$  for 5 min, and centrifuged at  $14000 \times g$  for 1 min. The final samples were boiled for 5 min before electrophoresis and protein immunoblot analysis.

### Tumor formation experiment in nude mice

From the selection of Anhui Medical University Animal Experiment Center, 4~6 weeks of nude mice were obtained. The treated cells were mixed with 50 μl matrix gel and 50 μl PBS solution and then slowly injected subcutaneously into the armpit of mice at  $1 \times 10^6$  cells. The body weight of the mice and the eruption of tumors under the armpit were observed daily, and vernier calipers recorded the tumor size. The mice have sacrificed appropriately, and the tumors were removed and weighed.

### Statistical methods

Results presented in figures were representative from triplicate. Data were expressed as mean ± standard deviation after analyzing with SPSS 26.0 Software (SPSS, Inc., USA). One-way ANOVA was used for comparison of statistical differences among multiple groups, followed by the LSD significant difference test. In case of comparison between two groups, an unpaired Student's *t*-test was used. Statistical significance was attributed at  $p < 0.05$ .

## Results

### Smoking promoted ΔNp63α expression in RCC patients and CSCs activity

To investigate the correlation between ΔNp63α expression and smoking status in patients with RCC, 20 patients were enrolled in this study, including 10 smokers and 10 non-smokers (Table 1). All patients were diagnosed as clear cell RCC and received radical nephrectomy in our center. Western blot analysis showed that ΔNp63α expression was significantly higher in smokers than non-smokers. The expression levels of RCSCs markers, CD44, Oct4, and SOX2 in smoking patients were remarkably higher than their counterparts (Figure 1A, Figure S1), which were consistent with outcomes of immunohistochemistry (Figure 1B).

### RCSCs were enriched by suspension culture using serum-free medium (SFM)

Renal cancer cells 786-O and ACHN were cultured in SFM and serum-supplied medium (SSM) for 5 days, respectively. We found that the morphology appearance of the cells in the SFM culture changed significantly from the original fusiform adherent growth to spherical suspension growth (Figure 2A). Then we investigated the alterations at the cellular and molecular level by analyzing the protein expression levels of RCSCs markers CD44, Oct4, and SOX2. As expected, the expression levels were significantly elevated in the SFM treatment group (Figure 2B). Moreover, qRT-PCR analyses revealed similar changes in the mRNA levels of RCSCs markers in the SFM treatment group (Figure 2C). In addition, flow cytometry of CD44-labeled renal cancer cells revealed a significant increase in CD44-positive cells (Figure 2D), confirming the apparent enrichment of RCSCs after SFM treatment again. Renal cancer cells cultured in SSM and SFM were collected and injected subcutaneously into the axilla of nude mice. Compared with the SSM group, the SFM group significantly increased the tumor size and weight (Figure 2E). Immunohistochemical results also showed that CD44

and ΔNp63α positive indicators in the SFM group were significantly increased, indicating that the activity of RCSCs was remarkably elevated (Figure 2F).

### CS promoted the activity of RCSCs

786-O and ACHN tumor spheres were treated with different concentrations of cigarette smoke extract (CSE) for 5 days, and cell viability was measured by CCK-8 assay. We found that cell viability enhanced significantly with increasing concentration, but cell viability began to decrease when the concentration exceeded 0.1% (Figure 3A). Therefore, we selected CSE concentrations of 0, 0.05%, and 0.1% for subsequent experimental treatment. It was discovered that the diameter and number of 786-O and ACHN tumor spheres were positively correlated with the increase of CSE concentration (Figure 3B). Next, we detected RCSCs treated with CS by western blot and qRT-PCR. Results showed that the protein (Figure 3C) and mRNA (Figure 3D) expression levels of RCSCs molecular markers were significantly elevated with the increase of CSE concentration. Moreover, a positive correlation between CSE concentration and the number of CD44-labeled positive cells was also detected by flow cytometry (Figure 3E). Furthermore, similar results were demonstrated *in vivo* (Figure 3F-G). Collectively, these results suggested that CS promoted the activity of RCSCs.

**Table 1** – Clinical characteristics of patients (n=20).

Parameters	Number of cases
Gender	
Male	14 (70%)
Female	6 (30%)
Age	
≤50	5 (25%)
>50~≤70	12 (60%)
>70	3 (15%)
Pack-years	
0	10 (50%)
>10~≤15	4 (20%)
>16	6 (30%)
Tumor size (cm)	
≤4	7 (35%)
>4~≤7	9 (45%)
>7	4 (20%)
Tumor stage	
pT1a	7 (35%)
pT1b	8 (40%)
pT2a	2 (10%)
pT2b	1 (5%)
pT3	2 (10%)
TNM stage	
I	15 (75%)
II	3 (15%)
III	2 (10%)
IV	0 (0%)

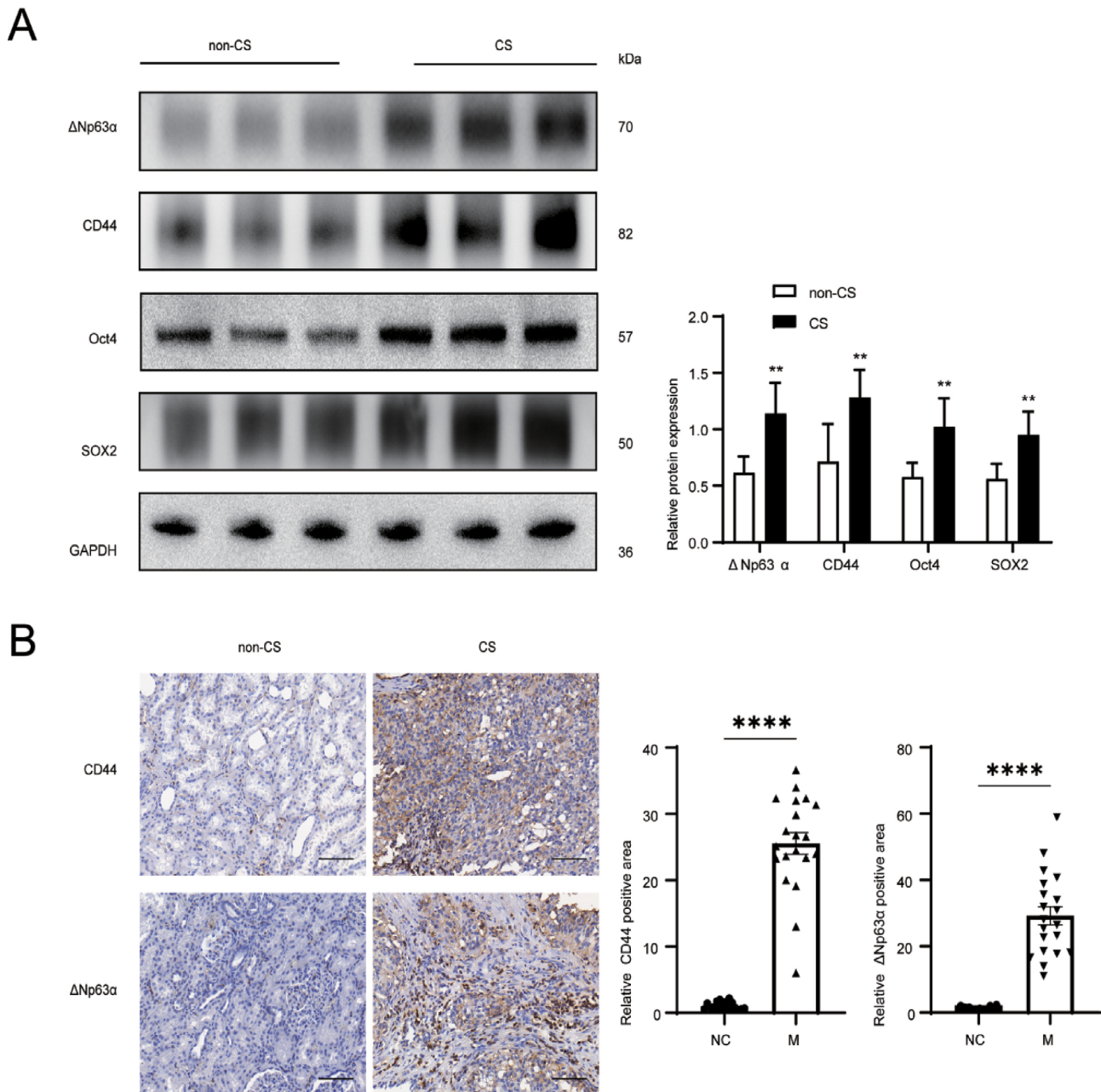


**Figure 1** – CS promotes the activity expression of  $\Delta$ Np63 $\alpha$  and CSCs markers in patients with kidney cancer. Western blot (A) and immunohistochemistry (B) detected the expression levels of  $\Delta$ Np63 $\alpha$  and RCSCs markers in the two groups (H&E, x200). \* $p$ <0.05, \*\* $p$ <0.01.

### $\Delta$ Np63 $\alpha$ facilitated CS-induced activity of RCSCs

Our results above have shown that  $\Delta$ Np63 $\alpha$  expression is closely associated with smoking status in renal cancer patients and  $\Delta$ Np63 $\alpha$  expression is high in 786-O and ACHN tumor spheres with CSE treatment (Figure 4A). To further investigate whether  $\Delta$ Np63 $\alpha$  plays a role in CS-induced RCSCs, the  $\Delta$ Np63 $\alpha$  plasmid was transfected into the CS-induced 786-O and ACHN tumor spheres, and the  $\Delta$ Np63 $\alpha$  overexpression model was established by culturing in an SFM medium for 4 days. Microscopy was performed to determine the cellular morphology alterations. We found that 786-O and ACHN tumor spheres were bigger in diameter and more numerous after plasmid transfection than those in the control group (Figure 4B). Moreover,  $\Delta$ Np63 $\alpha$  overexpression of 786-O and ACHN tumor spheres significantly increased the

protein expression levels of RCSCs markers CD44, Oct4, and SOX2 compared with the control group (Figure 4C). In contrast, the knockdown of  $\Delta$ Np63 $\alpha$  in tumor spheres with siRNA- $\Delta$ Np63 $\alpha$  resulted in a smaller tumor diameter and a reduced number of tumor spheres (Figure 4B). It suppressed the protein expression levels of RCSCs markers CD44, Oct4, and SOX2 (Figure 4D). These observations demonstrated a critical role of  $\Delta$ Np63 $\alpha$  in regulating the activity of RCSCs induced by CS.

### SHH signaling was stimulated in the CS-induced acquisition of activity in RCSCs

Western blot showed that the protein expression levels of Shh, Smo, Gli1, and Gli2 in 786-O and ACHN tumor spheres were increased after treatment with different concentrations

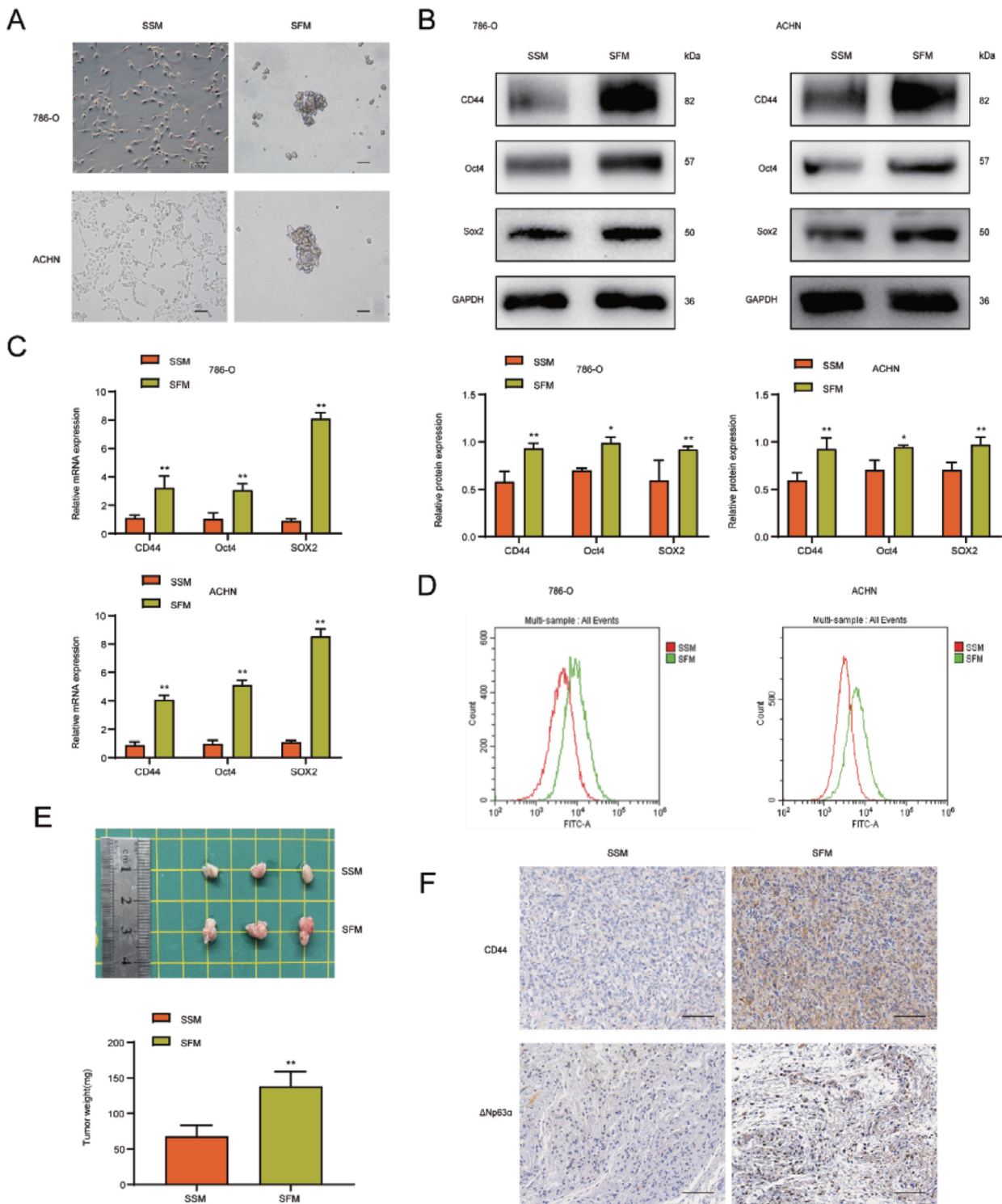


**Figure 2** – Enrichment of RCSCs by SFM. Renal cancer cells 786-O and ACHN were cultured with SFM and SFM for 5 days, respectively. (A) Microscopy was performed to observe the morphological changes of renal cancer cells (H&E, x100). The protein and mRNA expression levels of RCSCs markers were detected by western blot (B) and qRT-PCR (C). (D) The quantity of CD44-labeled positive cells in renal cancer cells was detected by flow cytometry. (E) Tumor size and weight were measured in SSM and SFM groups. (F) The expression of CD44 and ΔNp63α in SSM and SFM tissues was analyzed by immunohistochemistry (H&E, x200). \* $p < 0.05$ , \*\* $p < 0.01$ .

of CSE (Figure 5A), indicating the stimulation of the SHH signaling pathway. Then we explored the role of SHH signaling in CSE-induced RCSCs by using Vismodegib (Erivedge, Genentech, USA), an SHH signaling inhibitor, and found that Vismodegib treatment significantly reduced the size and

number of RCSCs spheroids (Figure 5B). Next, we detected that Vismodegib reduced protein expression of CD44, Oct4, and SOX2 in RCSCs 786-O and ACHN remarkably (Figure 5C). These results suggested that SHH signaling played a vital role in CSE-induced RCSCs.

### $\Delta$ Np63 $\alpha$ positively regulated CS-induced activity of RCSCs via the SHH pathway

To explore whether  $\Delta$ Np63 $\alpha$  regulates CS-induced activity of RCSCs through the SHH pathway, we transfected  $\Delta$ Np63 $\alpha$  overexpression plasmid and siRNA into CS-induced

786-O and ACHN tumorspheres. Western blot detected the expression levels of SHH signaling pathway-related proteins Shh, Smo, Gli1, and Gli2 in the transfected cells. As expected, the expression level of SHH signaling pathway-related proteins was increased in the overexpressed  $\Delta$ Np63 $\alpha$

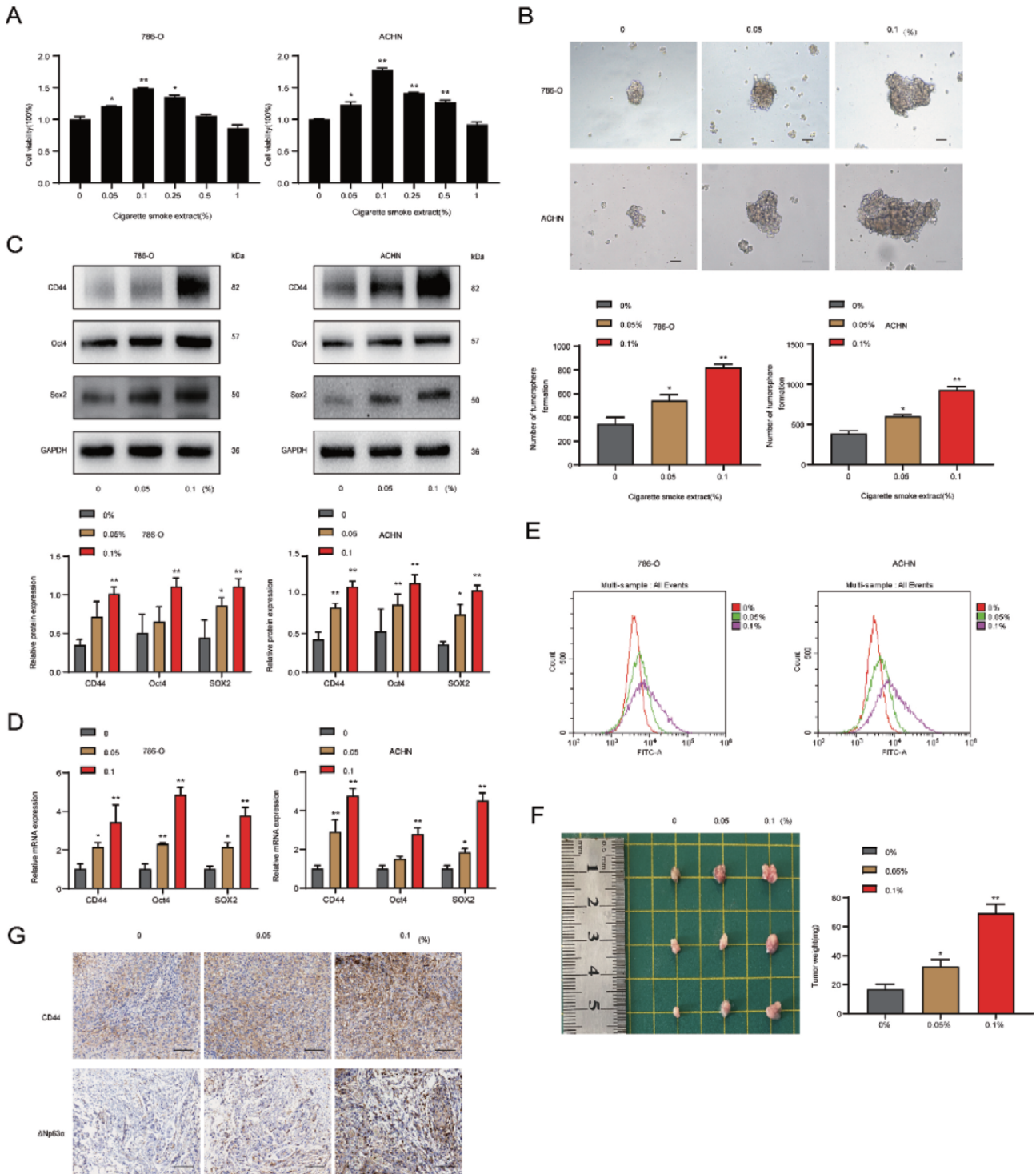
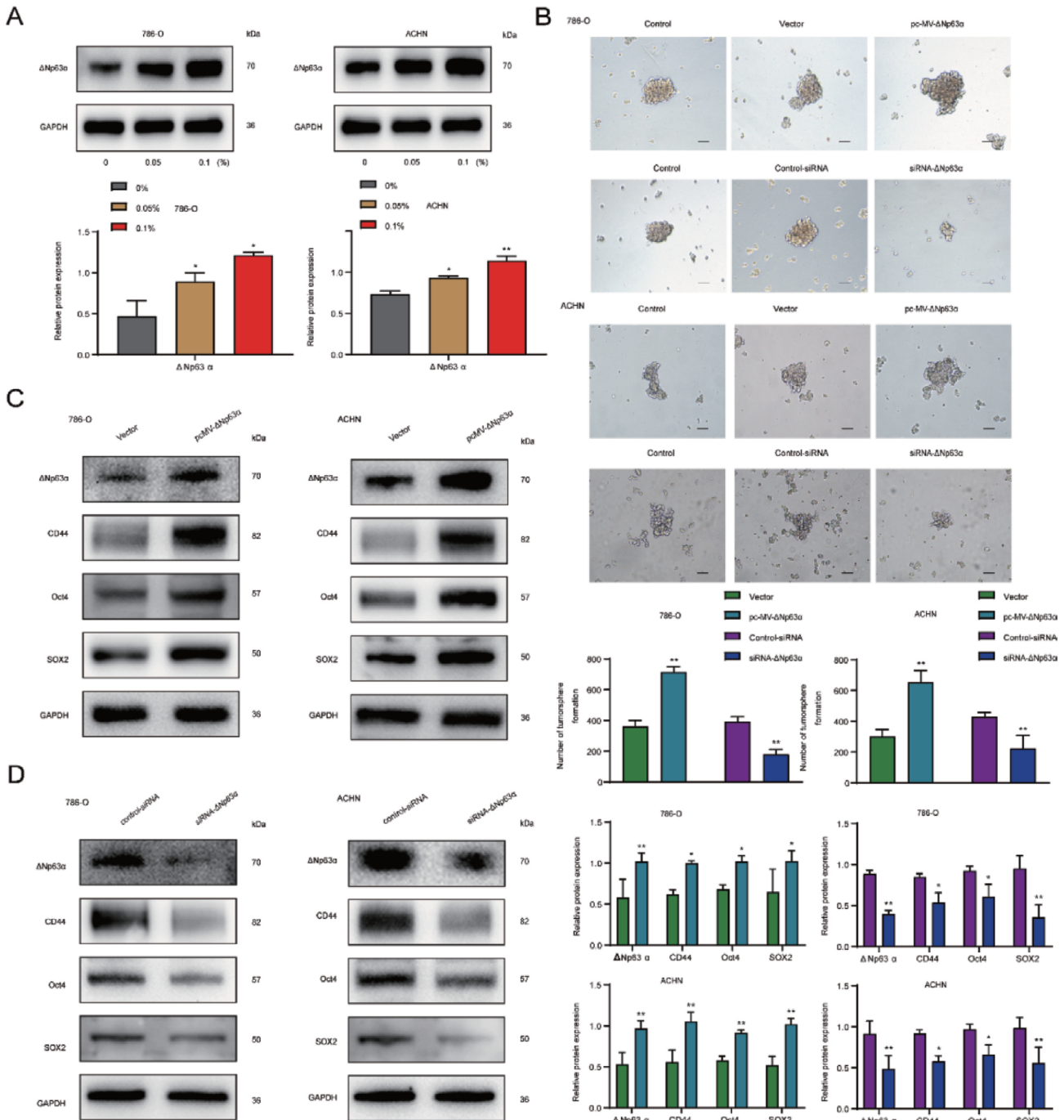


**Figure 3** – CS promotes the activity of RCSCs. RCSCs were administrated with various concentrations of CSE. (A) The effects of different concentrations of CSE on 786-O and ACHN tumor spheres were detected by CCK-8 assay. (B) The changes in the morphology and number of RCSCs treated with different concentrations of CSE were observed under a microscope (H&E, x100). The effects of CSE on the protein and mRNA expression levels of RCSCs markers were detected by western blot (C) and qRT-PCR (D). (E) Flow cytometry was utilized to determine the number of CD44-labeled positive cells in RCSCs treated with CSE. (F) The size and weight of tumors in the armpit of nude mice in the CSE-treated group were measured. (G) The immunohistochemical technique was used to detect the expression of CD44 and  $\Delta$ Np63 $\alpha$  in tumor tissues of the CSE-treated group (H&E, x200). \* $p < 0.05$ , \*\* $p < 0.01$ .

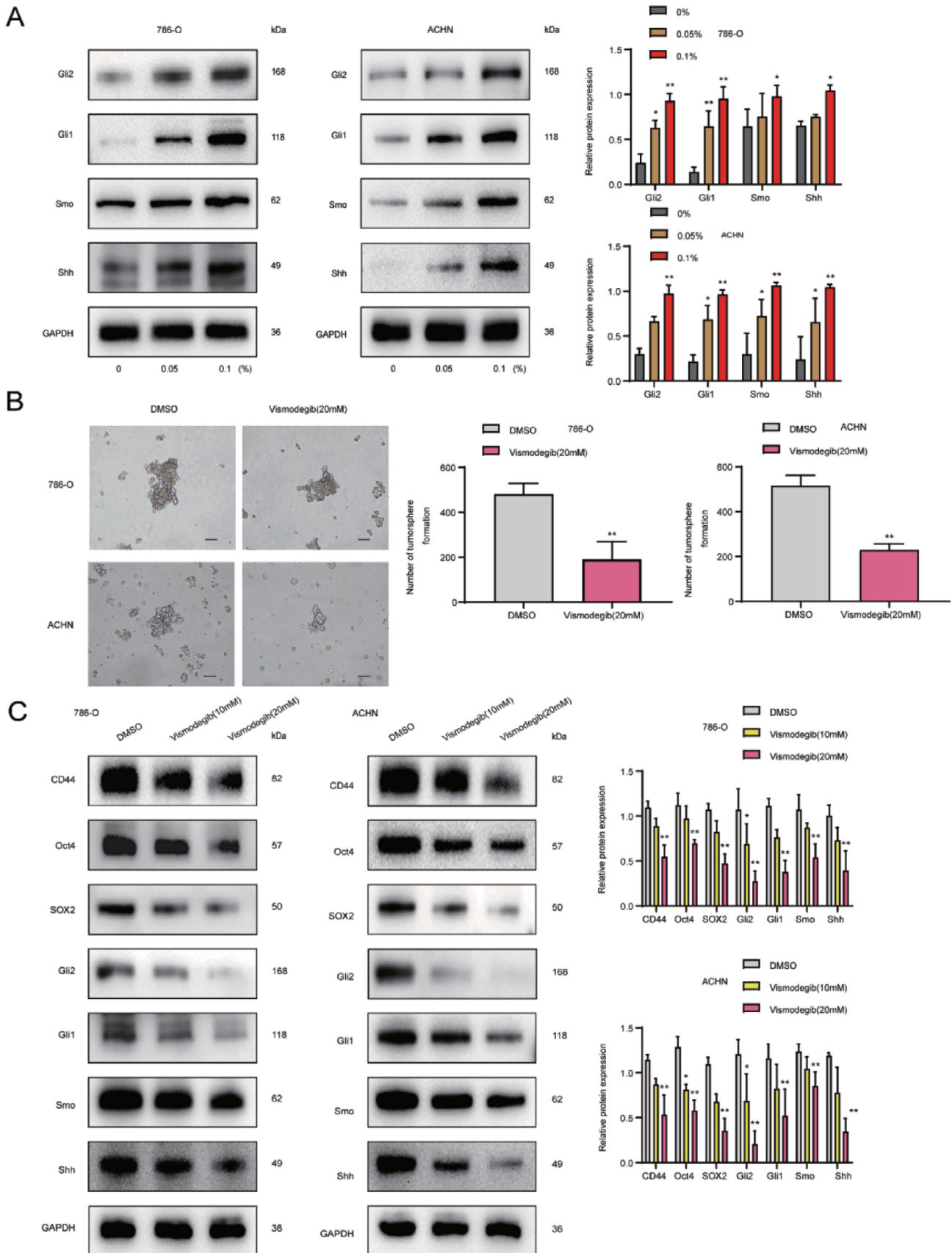
cells (Figure 6A). In contrast, inhibition of ΔNp63α reduced the expression of the SHH signaling pathway (Figure 6B). Subsequently, to verify this relationship, we performed a co-immunoprecipitation assay and verified the interaction of ΔNp63α with SHH signaling at the transcription level (Figure 6C). Figure 7 presents the mechanism involved in the CS-mediated induction through a schematic diagram. Our results revealed that ΔNp63α modulated CS-induced activity in RCSCs via the SHH pathway.

### Discussion

In recent years, the role of CSCs in the development and progression of RCC has been demonstrated (Lasorsa *et al.*, 2023). Ma *et al.* (2023) indicated that inhibition of the expression of a significant marker of CSCs, i.e., CD44, may be a new therapy to suppress ccRCC progression. Oct4, a stem cell transcription factor, and its overexpression was closely related to the progression of several malignancies, including ovarian cancer (Xie *et al.*, 2022), prostate cancer



**Figure 4** – ΔNp63α promotes CSE-induced activity in RCSCs. 786-O and ACHN tumor spheres were transfected with overexpression plasmids and targeted small interfering RNA. (A) Western blot analysis of ΔNp63α expression in CSE-treated tumorspheres. (B) Tumor spheres transfected with overexpression plasmid and siRNA were observed by microscopy (H&E, x200). (C) western blot analysis of the expression of ΔNp63α, CD44, Oct4, and SOX2 in tumorspheres transfected with overexpression plasmids. (D) Western blot analysis of the expression of ΔNp63α, CD44, Oct4, and SOX2 in the tumorspheres after siRNA transfection. \**p*<0.05, \*\**p*<0.01.





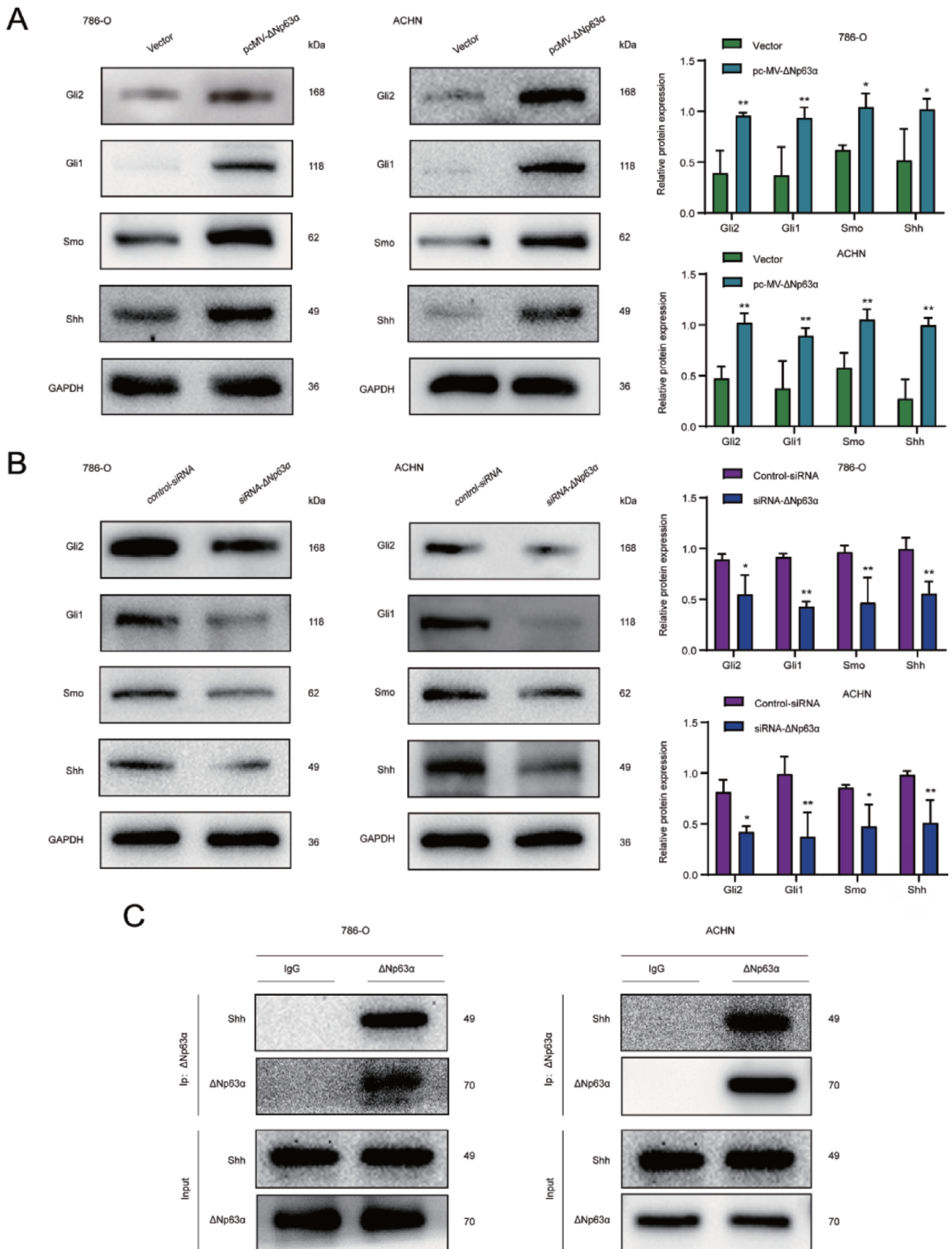


**Figure 6** –  $\Delta$ Np63 $\alpha$  positively regulates CS-induced activity in RCSCs through the SHH pathway. (A, B) Western blot was used to determine the expression levels of SHH signaling pathway-related proteins Shh, Smo, Gli1, and Gli2 in tumor spheres with or without  $\Delta$ Np63 $\alpha$  overexpression. (C) Co-immunoprecipitation assay examined the interaction between  $\Delta$ Np63 $\alpha$  and the SHH signaling pathway. \* $p$ <0.05, \*\* $p$ <0.01.

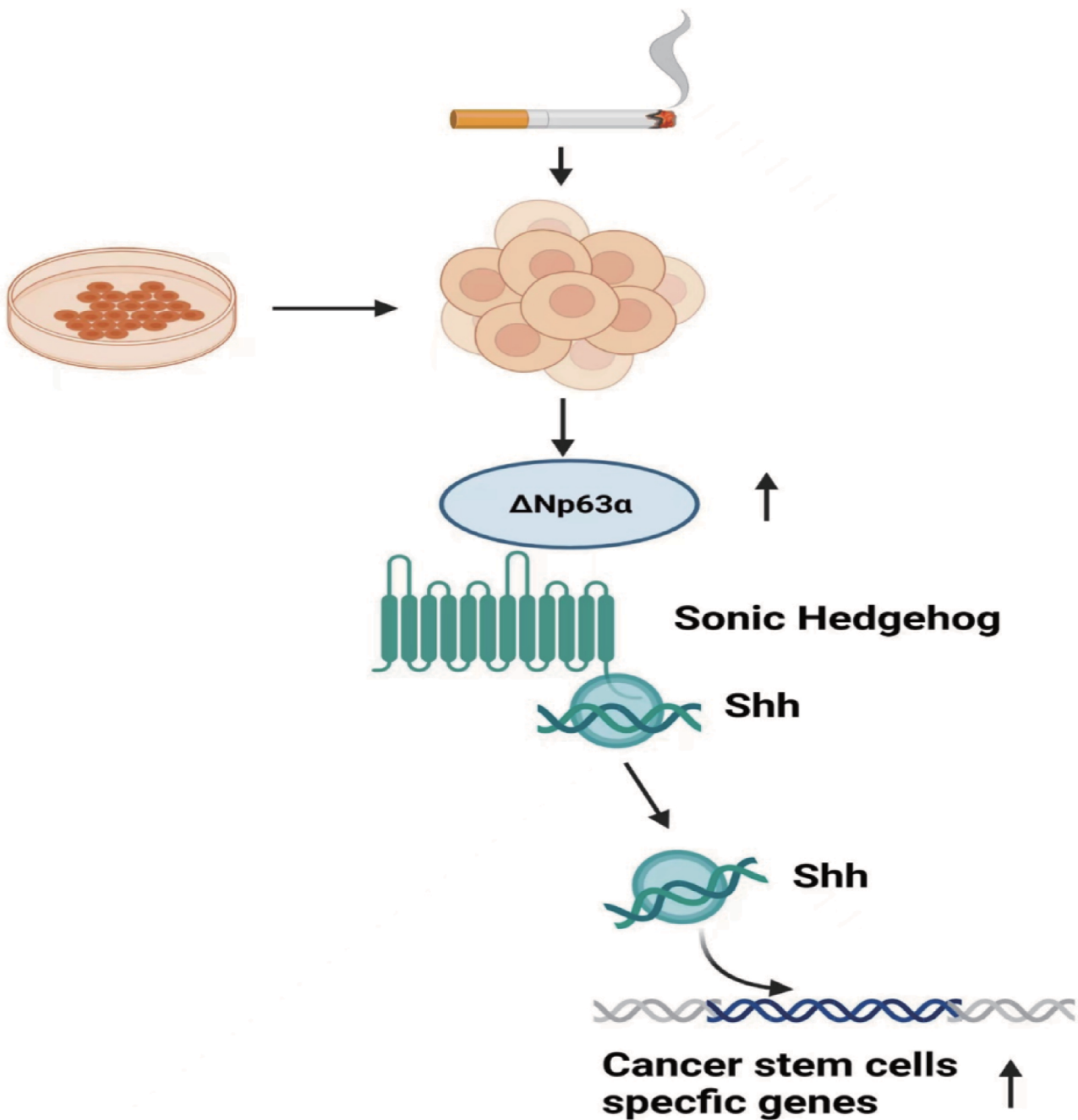


Figure 7 – Schematic diagram.

(Yasumizu *et al.*, 2020), and renal cancer (Zhang *et al.*, 2023). Overexpression of SOX2 is associated with cancer development, poor prognosis, and chemoresistance in several types of cancers (Mirzaei *et al.*, 2022). CS is an important risk factor of RCC.  $\Delta Np63\alpha$  has been demonstrated to be a vital RCC-associated gene. However, the molecular mechanism of  $\Delta Np63\alpha$  in CS-induced acquisition of activity in RCSCs remains unclear. We found that  $\Delta Np63\alpha$  expression in the RCC tissues of smokers was higher than that in the RCC tissues of non-smokers, and the levels of CSCs markers were significantly elevated in the RCC tissues of smokers.

In the presence of growth factors, culturing adherent cells in low-attachment plates with the serum-free medium

can improve tumorigenicity and enrich cell cultures with stem cell characteristics (House *et al.*, 2015). In this study, we cultured 786-O and ACHN renal cancer cells with SFM to increase spherical cells with stem cell characteristics, detected the expression levels of CSCs markers, and found that the protein expression levels of CSCs markers CD44, Oct4, and SOX2 increased. Flow cytometry showed that the number of CD44 labeled positive cells grew. Therefore, it is concluded that RCSCs are enriched after SFM treatment.

There is increasing evidence that CS can increase the activity of CSCs. CS contains various chemical components, among which nicotine is closely related to carcinogenesis (Li *et al.*, 2023). *In vitro*, we found that CS at a specific

concentration could increase the diameter and number of 786-O and ACHN tumor spheres, and the expression level of RCSCs markers (CD44, Oct4, SOX2) was significantly increased. *In vivo*, the tumor size and weight of nude mice increased after CSE treatment, and the expression of molecular markers of RCSCs was elevated. Our results suggested that CS promotes the stem cell activity of RCSCs.

$\Delta$ Np63 $\alpha$  overexpression plays a vital role in maintaining the activity of CSCs in several cancers (Cao *et al.*, 2008; Ge *et al.*, 2023). Cao *et al.* (2023) indicated that low-dose human phthalate exposure promoted the stem cell properties of breast CSCs in an  $\Delta$ Np63 $\alpha$  and SHH-dependent manner. The mechanism between CS and  $\Delta$ Np63 $\alpha$  has been poorly studied. In CS-exposed lung cancer cells,  $\Delta$ Np63 $\alpha$  regulated COX-2 expression and promoted inflammatory and tumorigenesis processes (Ratovitski, 2010).  $\Delta$ Np63 $\alpha$ /IRF6 interplay regulates nitric oxide synthase-2 transcription in head and neck squamous cell carcinoma cells and immortalized oral keratinocytes, which reveals its important role in the autophagy-related cancer cell response (Ratovitski, 2011).  $\Delta$ Np63 $\alpha$  promoted the acquisition of lung CSC-like properties in long-term tobacco smoke exposure-transformed Human bronchial epithelial cells (Xie *et al.*, 2019). However, the role of  $\Delta$ Np63 $\alpha$  in CS-induced RCSCs remains unknown. Our results showed increased  $\Delta$ Np63 $\alpha$  expression levels in RCC tissues from smokers.  $\Delta$ Np63 $\alpha$  overexpression enlarged tumor spheres in diameter and number and expressed higher levels of RCSCs markers. Moreover,  $\Delta$ Np63 $\alpha$  knockdown reduced tumor spheres in diameter and number and reduced the levels of RCSCs markers. These data revealed that  $\Delta$ Np63 $\alpha$  was essential for regulating stem cell activity in CS-induced RCSCs.

The SHH pathway plays a crucial role not only in embryonic organ development but also in the maintenance of CSC activity, tumorigenesis, metastasis, recurrence, and treatment (Jeng *et al.*, 2020). In breast cancer,  $\Delta$ Np63 $\alpha$  regulated the expression of Shh, SMO, Gli1, and Gli2 genes by directly binding to their gene regulatory regions and ultimately promoting the activation of signaling, whereas downregulation of  $\Delta$ Np63 $\alpha$  diminished SHH signaling molecules (Cao *et al.*, 2023). Similar findings were detected in RCC cells (Cao *et al.*, 2008). In this study, we observed that the protein expression levels of Shh, Smo, Gli1, and Gli2 were increased in 786-O and ACHN tumor spheres under CS treatment, and suppressed the ability of tumor sphere formation. The expression levels of CSCs markers were decreased after the administration of SHH signaling pathway inhibitor Vismodegib. Further studies found that  $\Delta$ Np63 $\alpha$  overexpression increased the expression of Shh, Smo, Gli1, and Gli2. Subsequent Co-IP experiments verified the interaction of  $\Delta$ Np63 $\alpha$  with the SHH signaling pathway. These observations demonstrated that  $\Delta$ Np63 $\alpha$  activated SHH signaling and promoted CS-induced activity in RCSCs.

The present study has several limitations. First, the small numbers of patients in the study might have led to possible selection bias. Second, other signaling pathways, Notch pathway for example, have also been found to be closely related to  $\Delta$ Np63 $\alpha$  and contribute to cancer progression, which warrants further study (Xie *et al.*, 2019).

## Conclusion

In conclusion, the present study demonstrated that  $\Delta$ Np63 $\alpha$  positively regulates the CS-induced activity of RCSCs via the SHH pathway, which may provide novel ideas and options for treatment of CS-related RCC.

## Acknowledgements

This work was supported by grants from the Natural Science Foundation of Anhui Province (No. 2008085MH290) and Anhui Medical University scientific research funds (Hefei, China; grant No. 2022xjk030, 2021xkj036).

## Conflict of Interest

The authors declare that there is no conflict of interest that could be perceived as prejudicial to the impartiality of the reported research.

## Author Contributions

XS,TZ conceived and designed the study; YZ, NM, WW, and YW conducted the experiments; WQ, WZ and XS analyzed the data; YZ and NM wrote the manuscript. All authors read and approved the final version.

## Data Availability

The data that support the findings of this study are available from the corresponding authors (zhangtao@ahmu.edu.cn or m15077916345\_1@163.com) upon reasonable request.

## References

- Behnsawy HM, Shigemura K, Meligy FY, Yamamichi F, Yamashita M, Haung WC, Li X, Miyake H, Tanaka K, Kawabata M *et al.* (2013) Possible role of sonic hedgehog and epithelial-mesenchymal transition in renal cell cancer progression. *Korean J Urol* 54:547-554.
- Cao WS, Zhao MJ, Chen Y, Zhu JY, Xie CF, Li XT, Geng SS, Zhong CY, Fu JY and Wu JS (2023) Low-dose phthalates promote breast cancer stem cell properties via the oncogene  $\Delta$ Np63 $\alpha$  and the Sonic hedgehog pathway. *Ecotoxicol Environ Saf* 252:114605.
- Cao Y, Wang L, Nandy D, Zhang Y, Basu A, Radisky D and Mukhopadhyay D (2008) Neuropilin-1 upholds dedifferentiation and propagation phenotypes of renal cell carcinoma cells by activating Akt and sonic hedgehog axes. *Cancer Res* 68:8667-8672.
- Ge M, Zhu J, Yi K, Chen Y, Cao W, Wang M, Xie C, Li X, Geng S, Wu J *et al.* (2023) Diallyl trisulfide inhibits gastric cancer stem cell properties through  $\Delta$ Np63/sonic hedgehog pathway. *Mol Carcinog* 62:1673-1685.
- House CD, Hernandez L and Annunziata CM (2015) *In vitro* enrichment of ovarian cancer tumor-initiating cells. *J Vis Exp* 96:52446.
- Jeng KS, Chang CF and Lin SS (2020) Sonic hedgehog signaling in organogenesis, tumors, and tumor microenvironments. *Int J Mol Sci* 21:758.
- Jubber I, Ong S, Bukavina L, Black PC, Compérat E, Kamat AM, Kiemeny L, Lawrentschuk N, Lerner SP, Meeks JJ *et al.* (2023) Epidemiology of bladder cancer in 2023: A systematic review of risk factors. *Eur Urol* 84:176-190.
- Lasorsa F, Rutigliano M, Milella M, Ferro M, Pandolfo SD, Crocetto F, Autorino R, Battaglia M, Ditunno P and Lucarelli G

- (2023) Cancer stem cells in renal cell carcinoma: Origins and biomarkers. *Int J Mol Sci* 24:13179.
- Li E, Zhang T, Sun X, Li Y, Geng H, Yu D and Zhong C (2019) Sonic hedgehog pathway mediates genistein inhibition of renal cancer stem cells. *Oncol Lett* 18:3081-3091.
- Li MY, Wang M, Dong M, Wu Z, Zhang R, Wang B, Huang Y, Zhang X, Zhou J, Yi J *et al.* (2023) Targeting CD36 determines nicotine derivative NNK-induced lung adenocarcinoma carcinogenesis. *iScience* 26:107477.
- Ma J, Wu R, Chen Z, Zhang Y, Zhai W, Zhu R and Zheng J (2023) CD44 Is a prognostic biomarker correlated with immune infiltrates and metastasis in clear cell renal cell carcinoma. *Anticancer Res* 43:3493-3506.
- Mirzaei S, Paskes MDA, Entezari M, Mirmazloomi SR, Hassanpoor A, Aboutalebi M, Rezaei S, Hejazi ES, Kakavand A, Heidari H *et al.* (2022) SOX2 function in cancers: Association with growth, invasion, stemness and therapy response. *Biomed Pharmacother* 156:113860.
- Qian W, Kong X, Zhang T, Wang D, Song J, Li Y, Li X, Geng H, Min J, Kong Q *et al.* (2018) Cigarette smoke stimulates the stemness of renal cancer stem cells via Sonic Hedgehog pathway. *Oncogenesis* 7:24.
- Ratovitski EA (2010) LKB1/PEA3/ $\Delta$ Np63 pathway regulates PTGS-2 (COX-2) transcription in lung cancer cells upon cigarette smoke exposure. *Oxid Med Cell Longev* 3:317-324.
- Ratovitski EA (2011)  $\Delta$ Np63 $\alpha$ /IRF6 interplay activates NOS2 transcription and induces autophagy upon tobacco exposure. *Arch Biochem Biophys* 506:208-215.
- Rouprêt M, Seisen T, Birtle AJ, Capoun O, Compérat EM, Dominguez-Escrig JL, Gürses Andersson I, Liedberg F, Mariappan P, Hugh Mostafid A *et al.* (2023) 404 European Association of Urology Guidelines on upper urinary tract urothelial carcinoma: 2023 Update. *Eur Urol* 84:49-64.
- Wu B, Shi X, Jiang M and Liu H (2023) Cross-talk between cancer stem cells and immune cells: Potential therapeutic targets in the tumor immune microenvironment. *Mol Cancer* 22:38.
- Xia C, Dong X, Li H, Cao M, Sun D, He S, Yang F, Yan X, Zhang S, Li N *et al.* (2022) Cancer statistics in China and United States, 2022: Profiles, trends, and determinants. *Chin Med J (Engl)* 135:584-590.
- Xie C, Zhu J, Jiang Y, Chen J, Wang X, Geng S, Wu J, Zhong C, Li X and Meng Z (2019) Sulforaphane inhibits the acquisition of tobacco smoke-induced lung cancer stem cell-like properties via the IL-6/ $\Delta$ Np63 $\alpha$ /Notch Axis. *Theranostics* 9:4827-4840.
- Xie W, Yu J, Yin Y, Zhang X, Zheng X and Wang X (2022) OCT4 induces EMT and promotes ovarian cancer progression by regulating the PI3K/AKT/mTOR pathway. *Front Oncol* 12:876257.
- Yasumizu Y, Rajabi H, Jin C, Hata T, Pitroda S, Long MD, Hagiwara M, Li W, Hu Q, Liu S *et al.* (2020) MUC1-C regulates lineage plasticity driving progression to neuroendocrine prostate cancer. *Nat Commun* 11:338.
- Yuan S, Chen J, Ruan X, Sun Y, Zhang K, Wang X, Li X, Gill D, Burgess S, Giovannucci E *et al.* (2023) Smoking, alcohol consumption, and 24 gastrointestinal diseases: Mendelian randomization analysis. *Elife* 12:e84051.
- Zhang T, Cao W, Sun H, Yu D and Zhong C (2023) Diallyl trisulfide suppresses the renal cancer stem-like cell properties via Nanog. *Nutr Cancer* 75:971-979.
- Zhang T, Zhao L, Zhang T, Wu W, Liu J, Wang X, Wan Y, Geng H, Sun X, Qian W *et al.* (2020) Curcumin negatively regulates cigarette smoke-induced renal cell carcinoma epithelial-mesenchymal transition through the ERK5/AP-1 pathway. *Onco Targets Ther* 13:9689-9700.
- Znaor A, Lortet-Tieulent J, Laversanne M, Jemal A and Bray F (2015) International variations and trends in renal cell carcinoma incidence and mortality. *Eur Urol* 67:519-530.

## Supplementary material

The following online material is available for this article:

Figure S1 – Western blot analysis of the expression levels of RCSCs markers, CD44, Oct4, and SOX2 in clinical patients.

*Associate Editor: Daisy Maria Fávero Salvadori*

License information: This is an open-access article distributed under the terms of the Creative Commons Attribution License (type CC-BY), which permits unrestricted use, distribution and reproduction in any medium, provided the original article is properly cited.